Electronic Supplementary Material (ESI) for New Journal of Chemistry

Theoretical Prediction of Chiral Actinide Endohedral Borospherenes

Naixin Zhang,[‡a,b] *Ailin Li,*[‡a,b] *Cong-Zhi Wang,**[a] *Qun-Yan Wu,*[a] *Jian-Hui Lan,*[a] *Zhi-Fang Chai,*[a,c] *Yu-Bao Zhao,*[b] *and Wei-Qun Shi**[a]

[a]Laboratory of Nuclear Energy Chemistry, Institute of High Energy Physics, Chinese Academy of Sciences, Beijing 100049, China

[b]School of Chemistry and Chemical Engineering, University of South China, Hengyang 421001, China

[c]Engineering Laboratory of Advanced Energy Materials, Ningbo Institute of Industrial Technology, Chinese Academy of Sciences, Ningbo, Zhejiang, 315201, China

[‡]The first two authors contributed equally to this work.

Email: shiwq@ihep.ac.cn, wangcongzhi@ihep.ac.cn

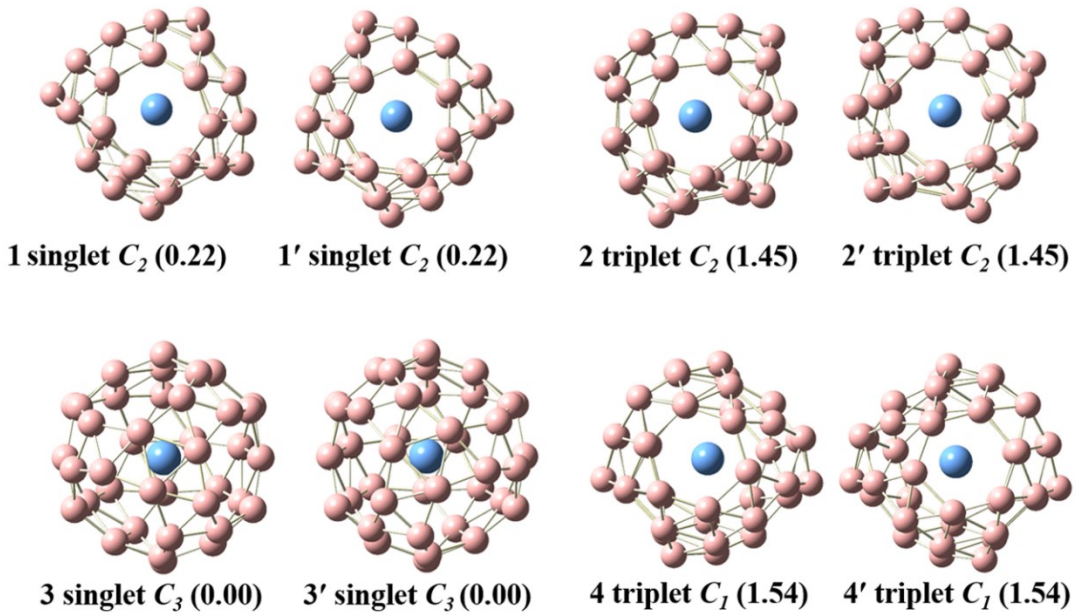

Figure S1. Low-lying isomers of $[Ac@B_{39}]^{2+}$ with the relative energies (eV) at the PBE0/RECP/6-311+G* levels. Light pink and blue spheres represent B and Ac, respectively. All the energies have been corrected for zero-point energies.

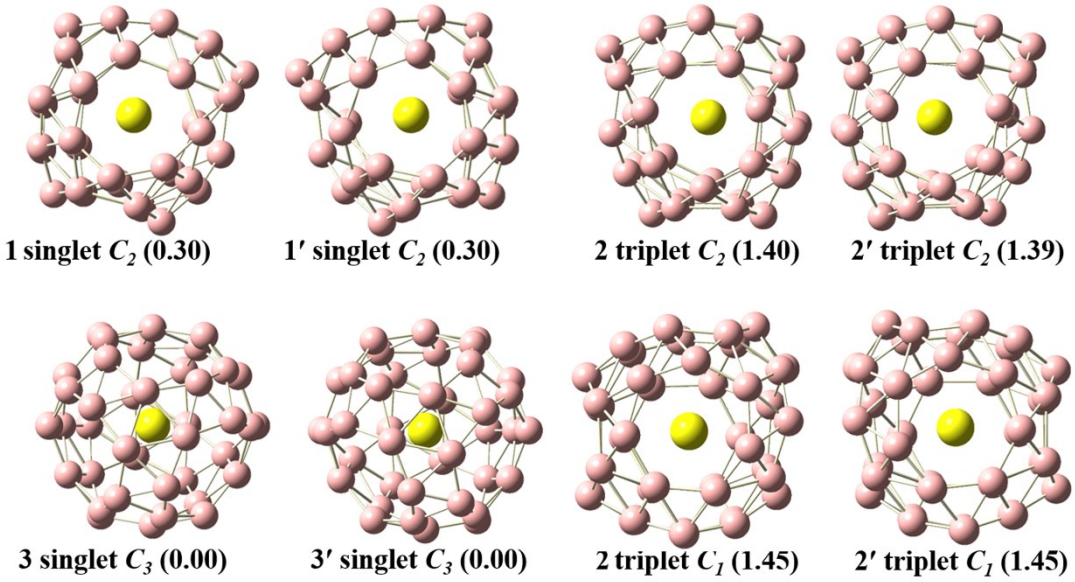

Figure S2. Low-lying isomers of $[Th@B_{39}]^{3+}$ with the relative energies (eV) at the PBE0/RECP/6-311+G* levels. Light pink and yellow spheres represent B and Th, respectively. All the energies have been corrected for zero-point energies.

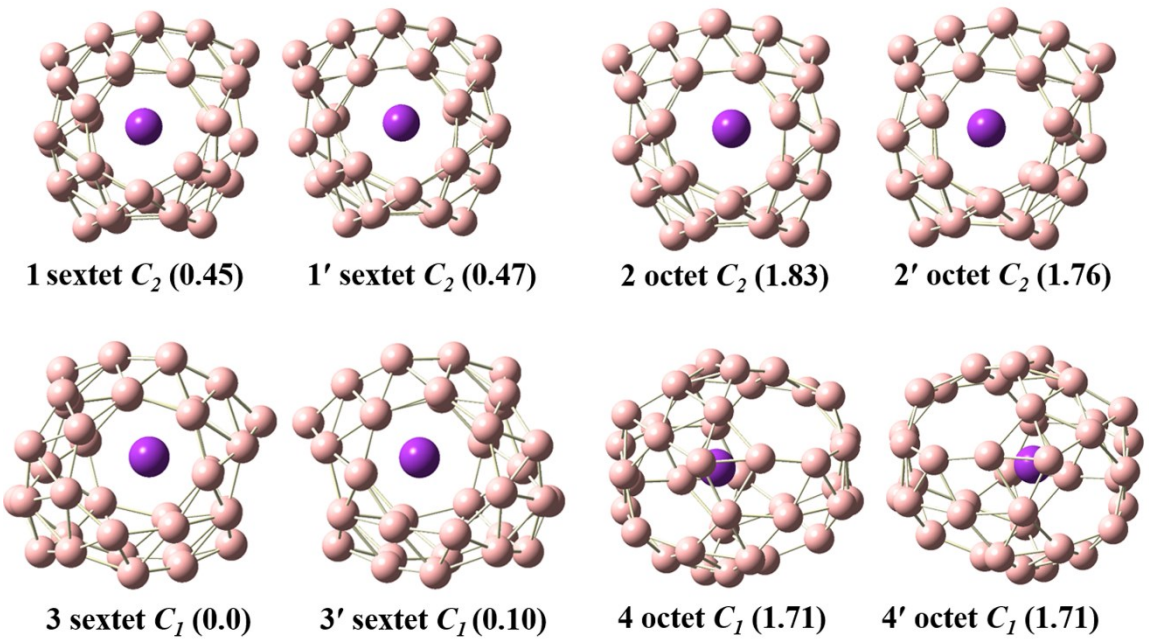

Figure S3. Low-lying isomers of $[Cf@B_{39}]^{2+}$ with the relative energies (eV) at the PBE0/RECP/6-311+G* levels. Light pink and yellow spheres represent B and Th, respectively. All the energies have been corrected for zero-point energies.

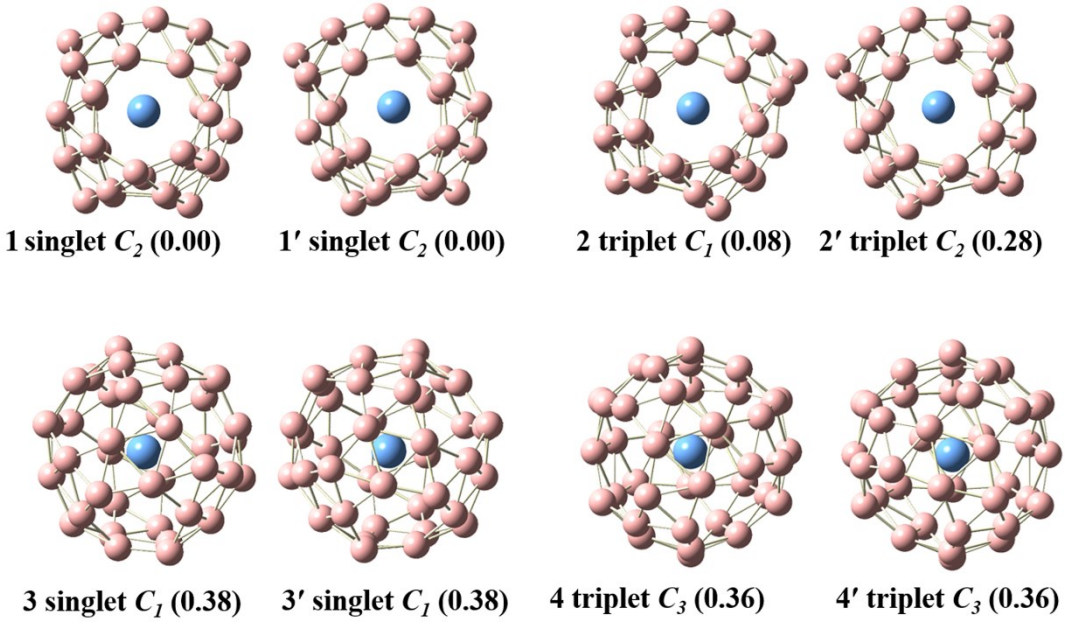

Figure S4. Low-lying isomers of $Ac@B_{39}$ with the relative energies (eV) at the PBE0/RECP/6-311+G* levels. Light pink and blue spheres represent B and Ac, respectively. All the energies have been corrected for zero-point energies.

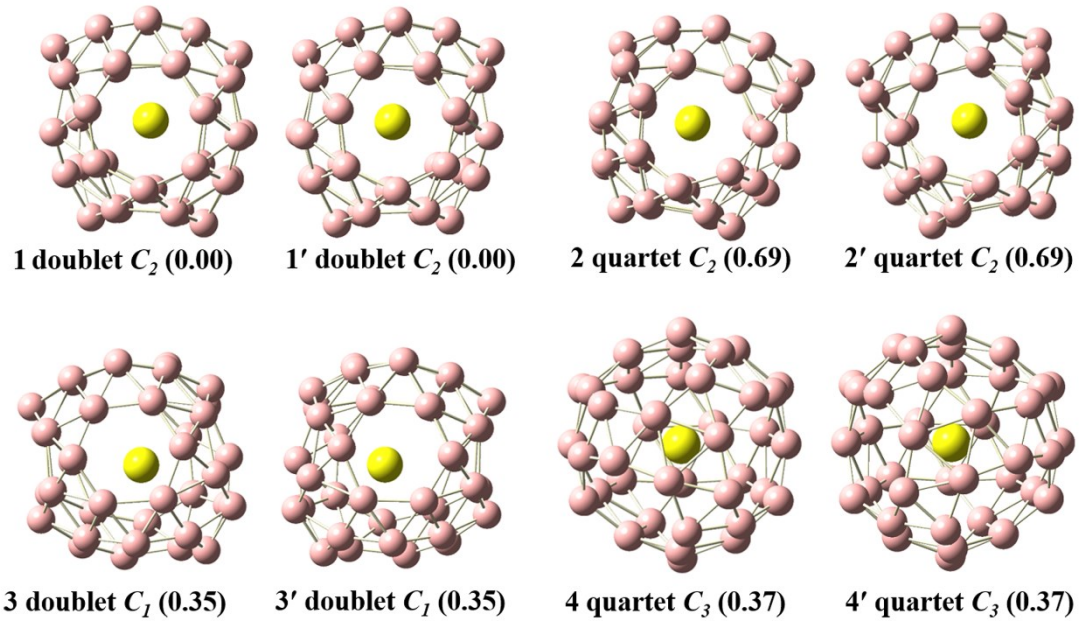

Figure S5. Low-lying isomers of Th@B_{39} with the relative energies (eV) at the PBE0/RECP/6-311+G* levels. Light pink and yellow spheres represent B and Th, respectively. All the energies have been corrected for zero-point energies.

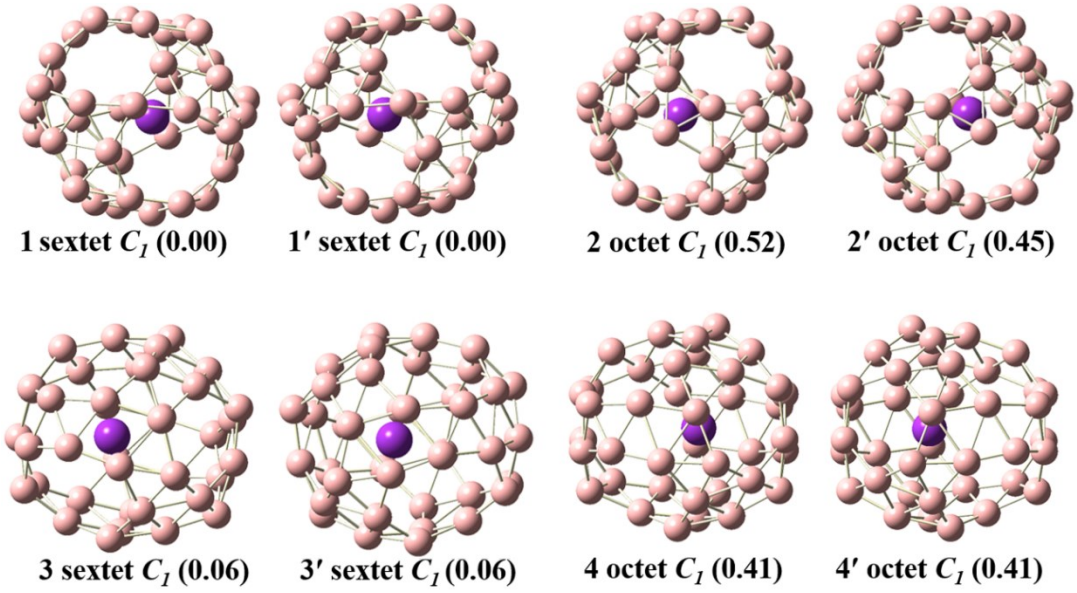

Figure S6. Low-lying isomers of Cf@B_{39} with the relative energies (eV) at the PBE0/RECP/6-311+G* levels. Light pink and yellow spheres represent B and Th, respectively. All the energies have been corrected for zero-point energies.

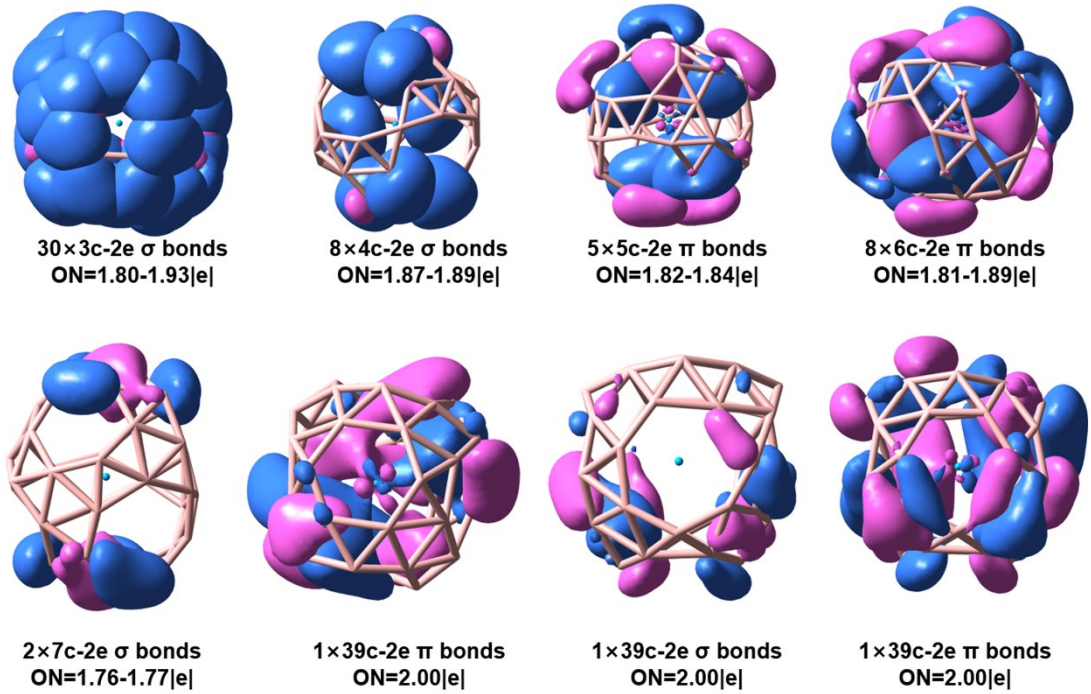

Figure S7. Bonding pattern of C_2 $[Th@B_{39}]^{3+}$ from AdNDP analysis with the occupation numbers (ONs) indicated at the PBE0/6-311+G*/RECP level of theory.

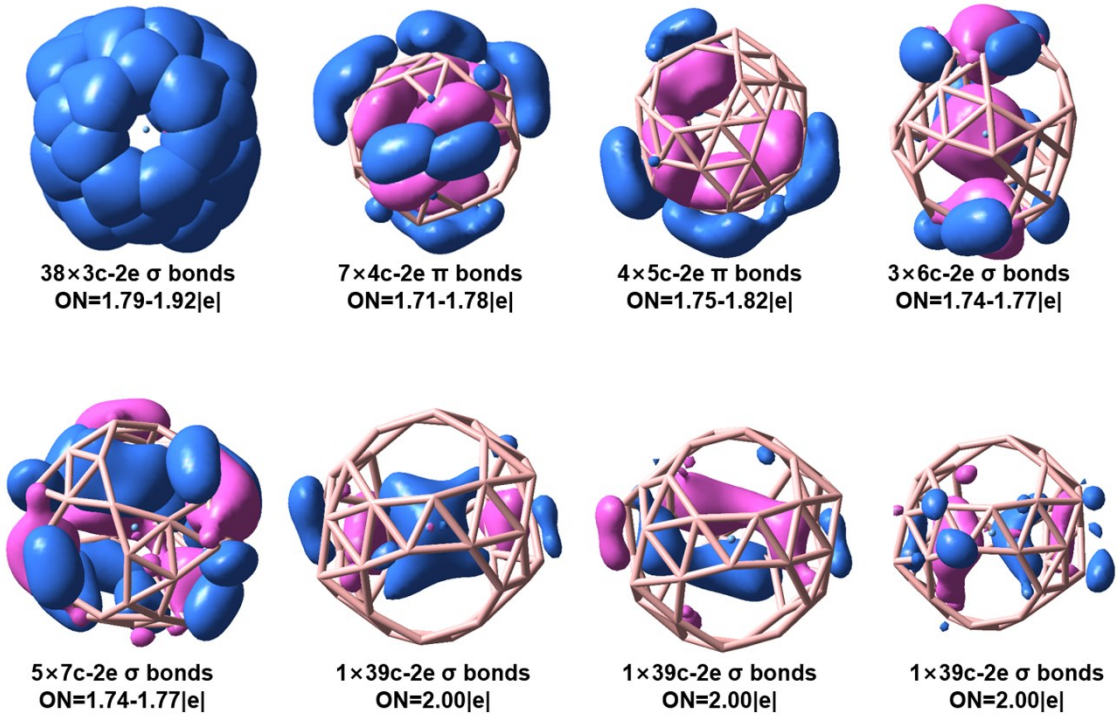

Figure S8. Bonding pattern of C_2 $Ac@B_{39}$ from AdNDP analysis with the ONs indicated at the PBE0/6-311+G*/RECP level of theory.

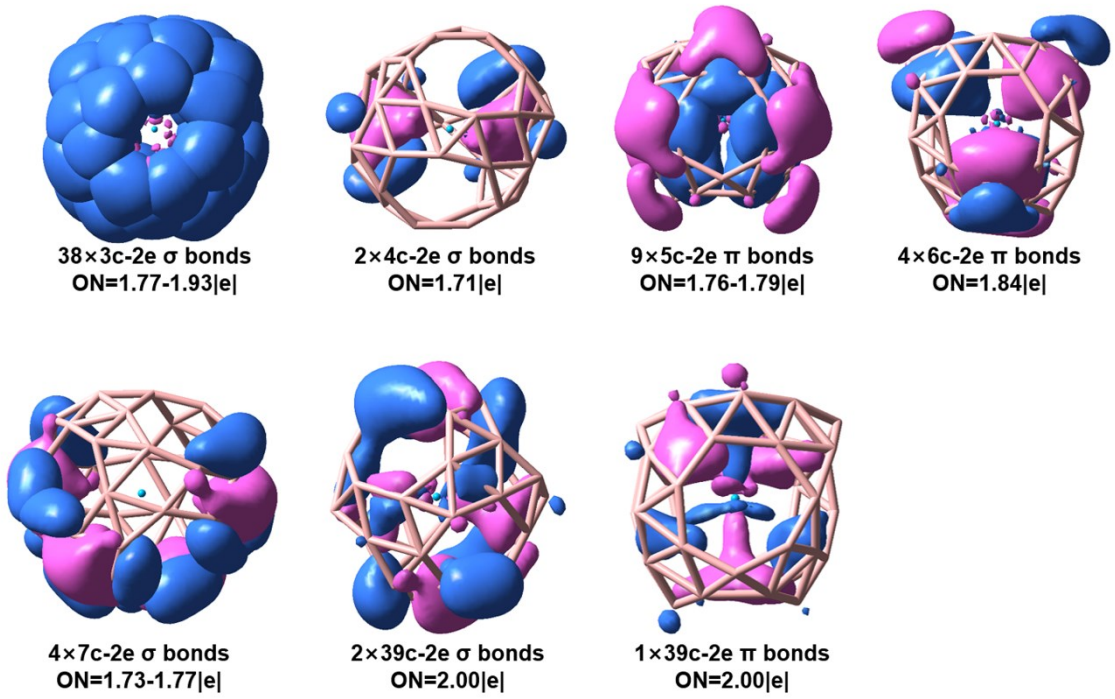

Figure S9. Bonding pattern of C_2 Th@B_{39} from AdNDP analysis with the ONs indicated at the PBE0/6-311+G*/RECP level of theory.

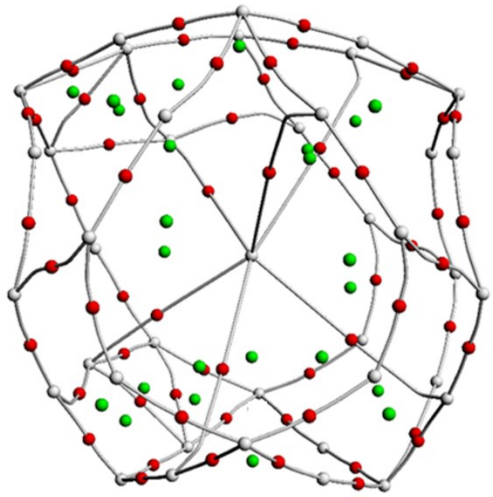

Figure S10. QTAIM analysis of C_2 $[Th@B_{39}]^{3+}$ at the PBE0/6-311+G*/RECP level of theory. Red points represent bond critical points, gray lines represent bond paths. Green points represent ring critical points, blue points represent cage critical points.

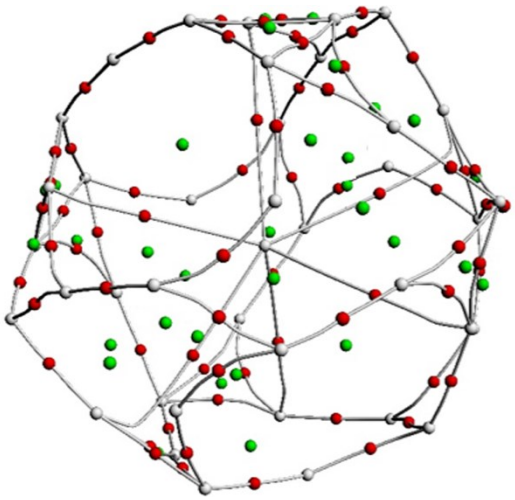

Figure S11. QTAIM analysis of C_2 Ac@B_{39} at the PBE0/6-311+G*/RECP level of theory.

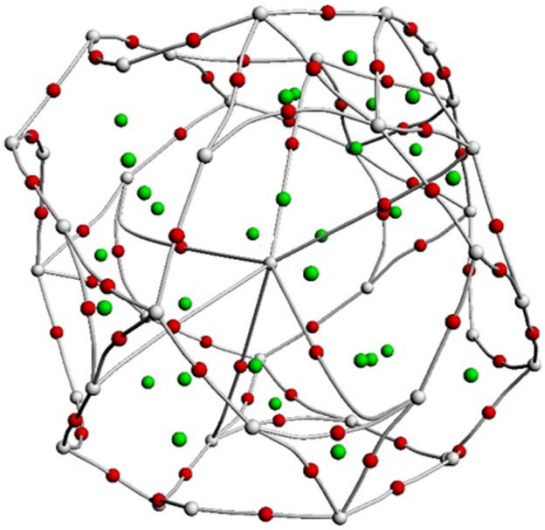

Figure S12. QTAIM analysis of C_2 Th@B_{39} at the PBE0/6-311+G*/RECP level of theory.

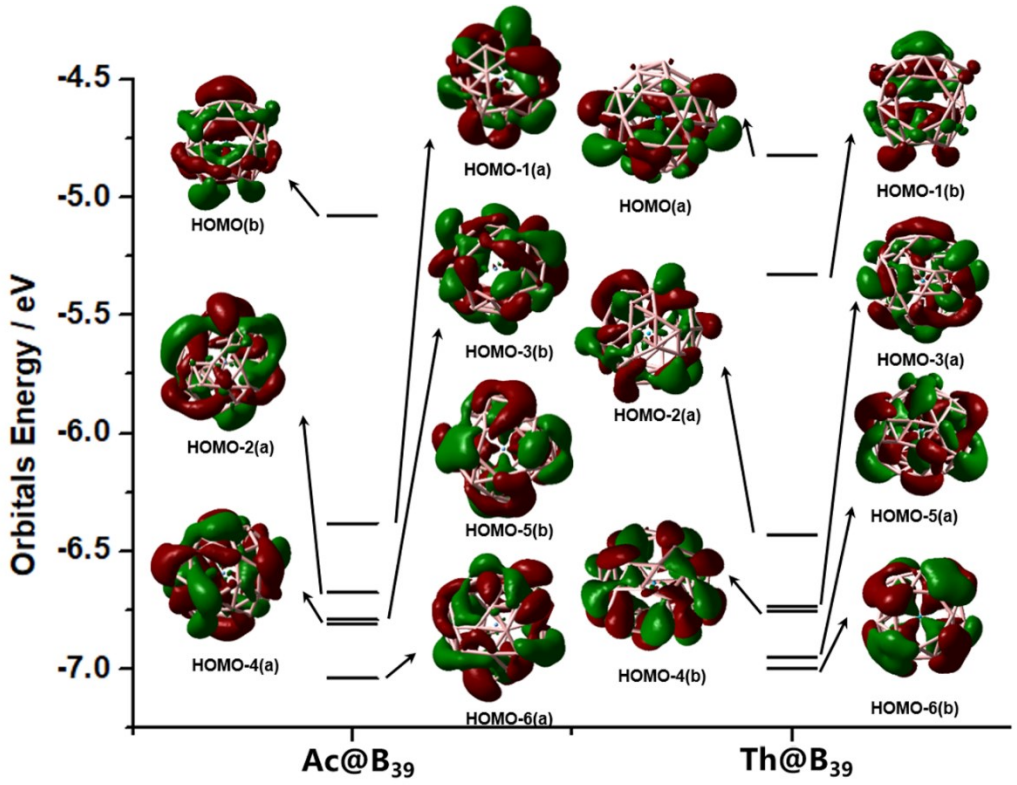

Figure S13. The frontier molecular orbitals of $Ac@B_{39}$ and $Th@B_{39}$ at the PBE0/6-311+G*/RECP level of theory.

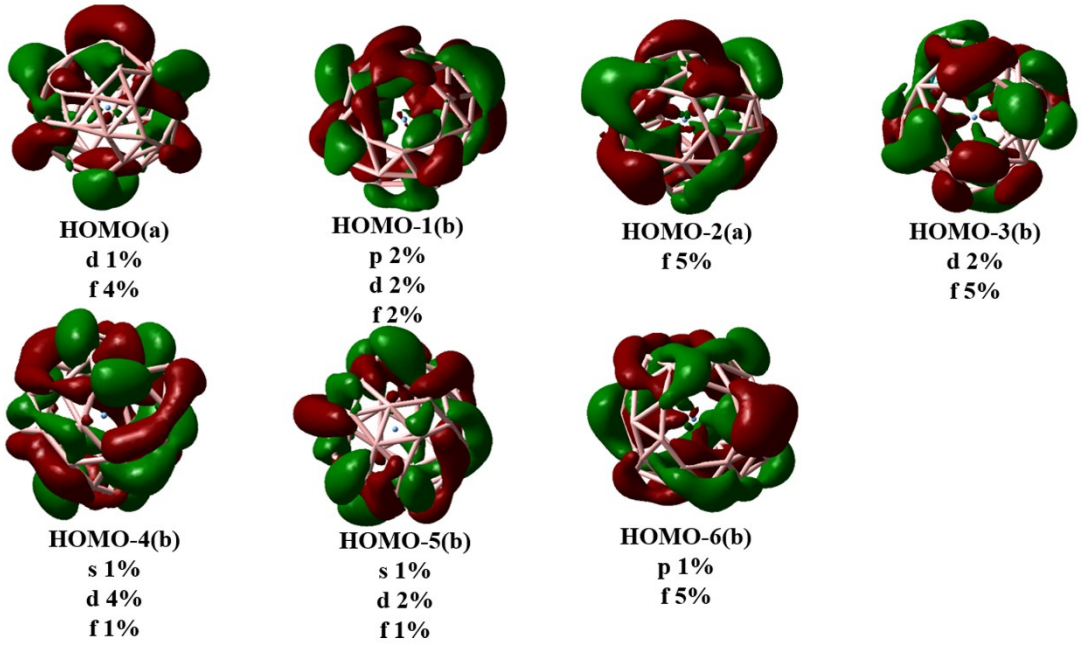

Figure S14. The composition of MO for $[Ac@B_{39}]^{2+}$ at the PBE0/6-311+G*/RECP level of theory.

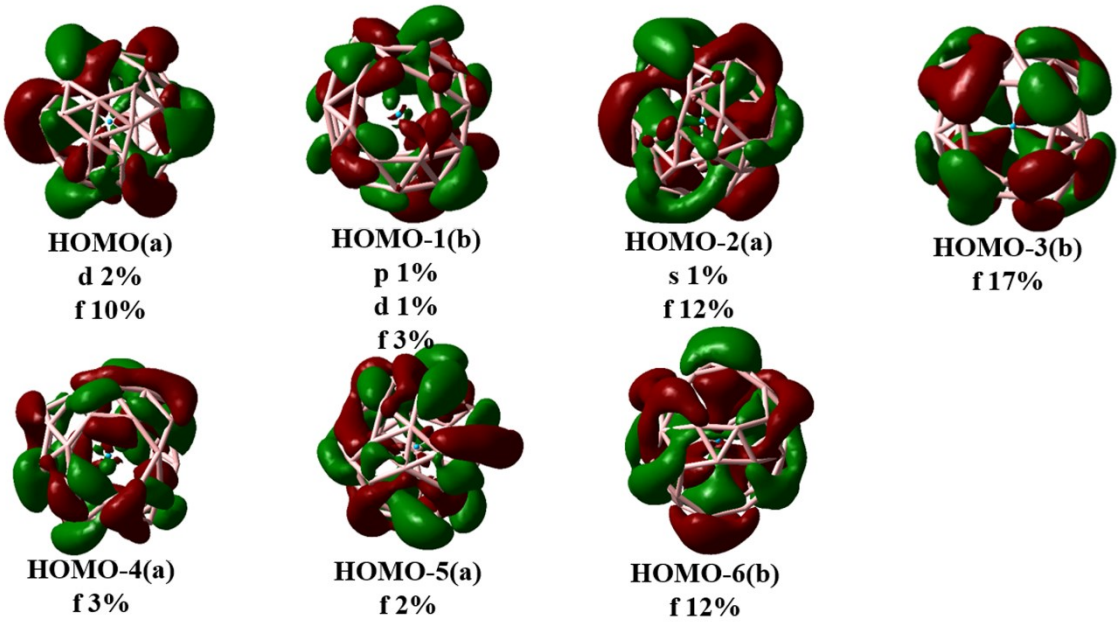

Figure S15. The composition of MO for $[Th@B_{39}]^{3+}$ at the PBE0/6-311+G*/RECP level of theory.

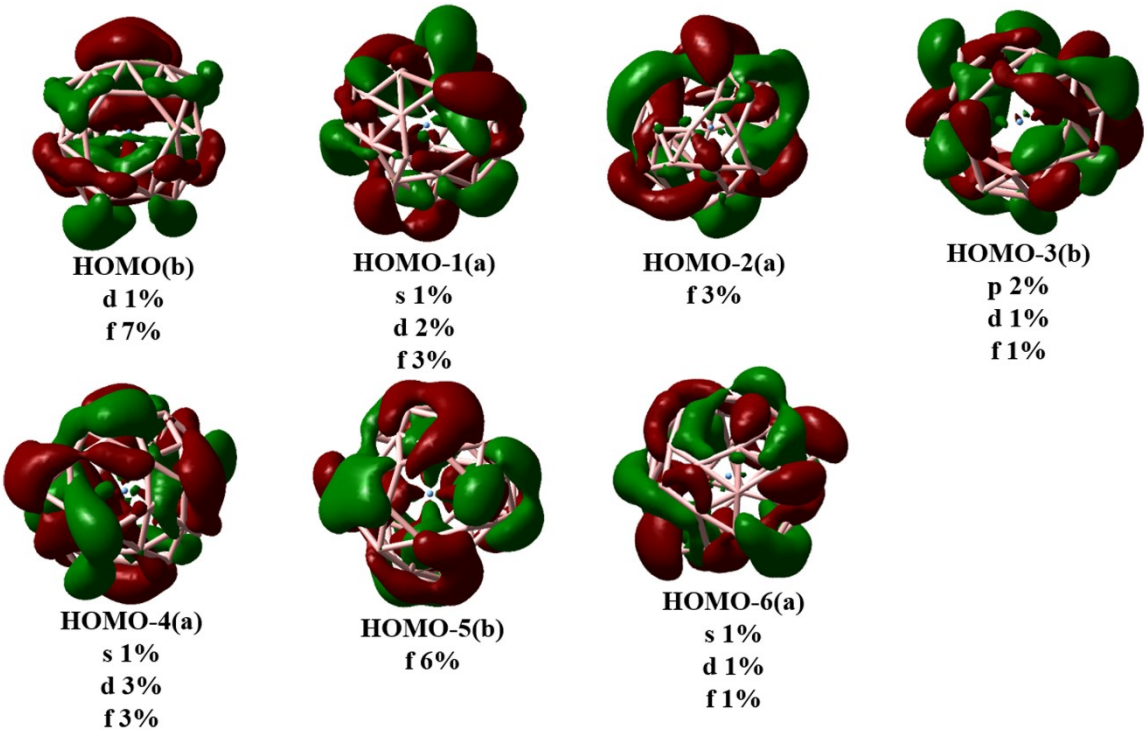

Figure S16. The composition of MO for $Ac@B_{39}$ at the PBE0/6-311+G*/RECP level of theory.

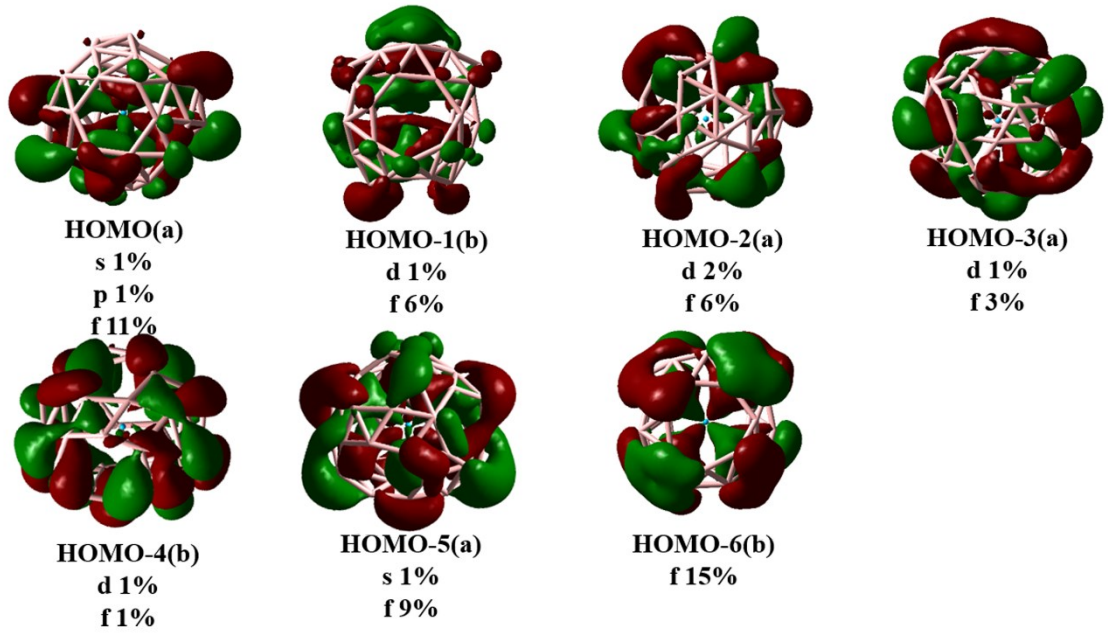

Figure S17. The composition of MO for Th@B_{39} at the PBE0/6-311+G*/RECP level of theory.

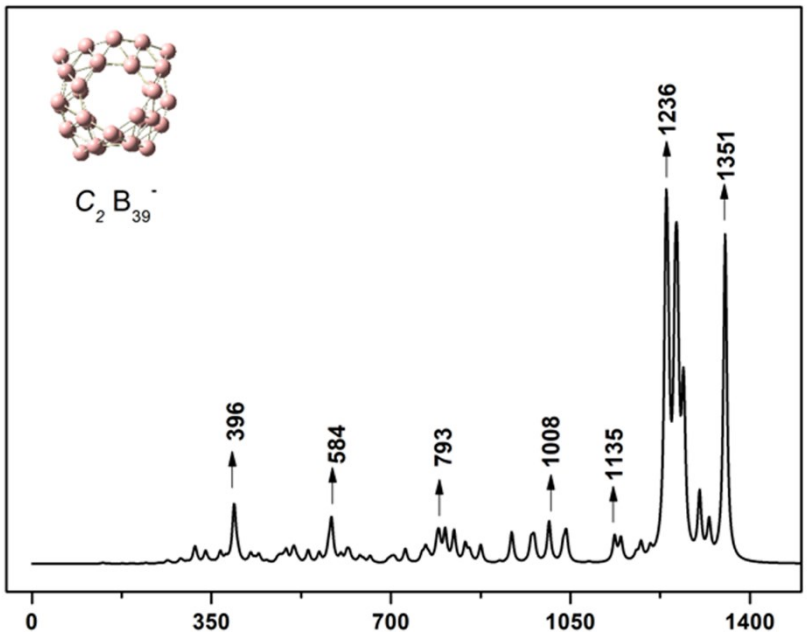

Figure S18. The infrared spectra of $C_2B_{39}^-$ at the PBE0/6-311+G*/RECP level of theory.

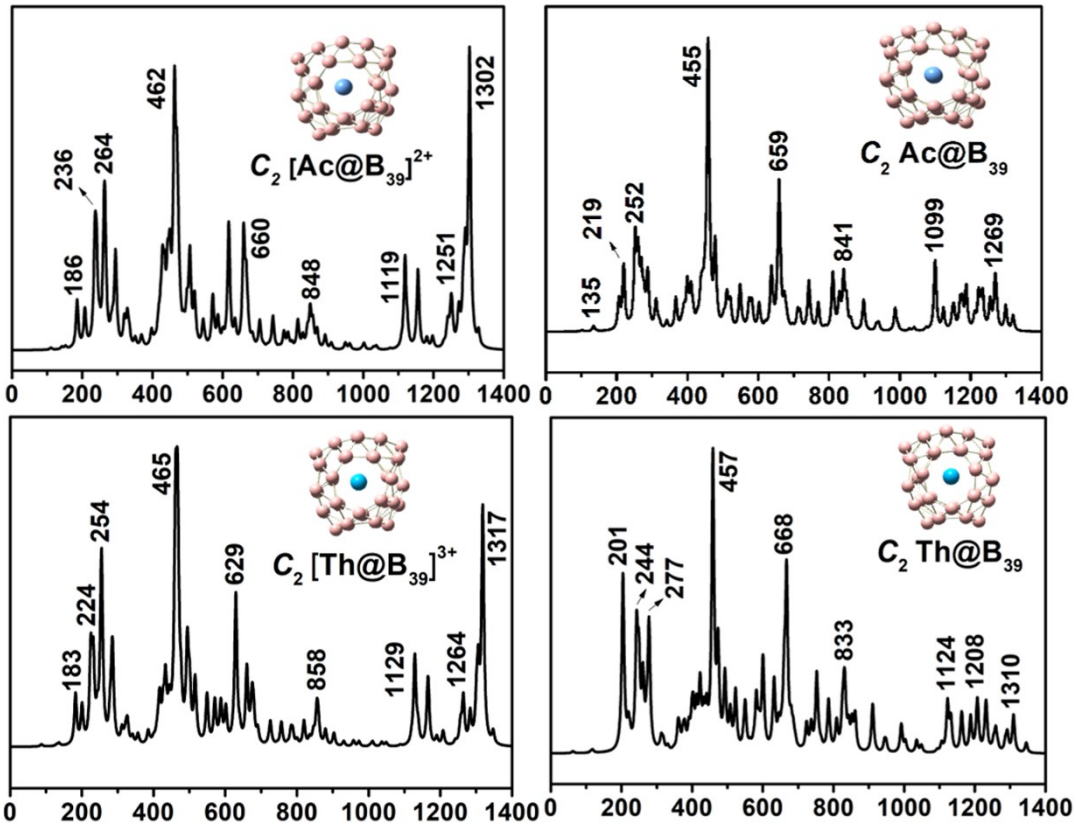

Figure S19. The Raman spectra of $[An@B_{39}]^{n+}$ at the PBE0/6-311+G*/RECP level of theory.

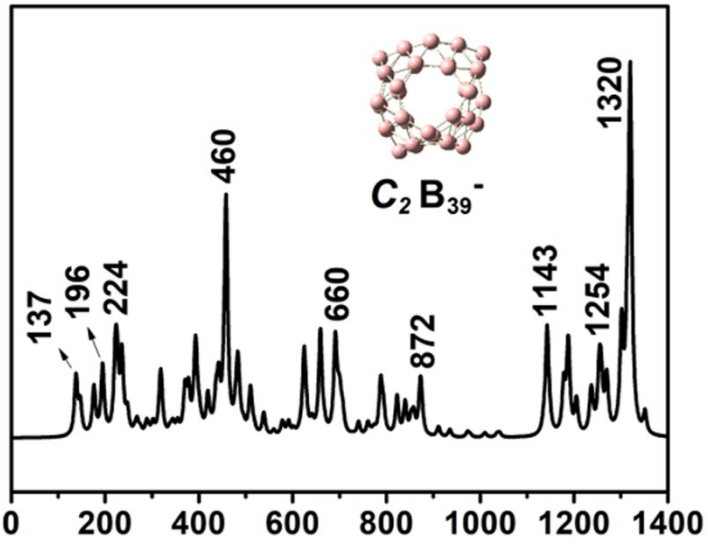

Figure S20. The Raman spectra of C_2 B_{39}^- at the PBE0/6-311+G*/RECP level of theory.

Table S1. Mayer bond orders (MBOs) of the An-B bonds for $[An@B_{39}]^{n+}$ calculated by the PBE0 method.

Species	MBOs	Total MBOs
C_2 $[Ac@B_{39}]^{2+}$	0.022 - 0.119	2.168
C_2 $Ac@B_{39}$	0.048 - 0.115	3.230
C_2 $[Th@B_{39}]^{3+}$	0.146 - 0.304	7.352
C_2 $Th@B_{39}$	0.140 - 0.264	6.898

Table S2. The EDA results (kcal/mol) of $Th@B_{39}$ with Th^{4+} and B_{39}^{4-} as the two fragments at the PBE/TZP/ZORA level of theory.

Species	ΔE_{Pauli}	ΔE_{elstat}	ΔE_{steric}	ΔE_{orb}	ΔE_{int}
$Th@B_{39}$	212.5	-1076.5 (49.9%)	-864.0	-1079.5 (50.1%)	-1943.5

Table S3. In the QTAIM analysis of C_2 $[Ac@B_{39}]^{2+}$, density of electrons ρ, energy density H(r), Laplacian of electron density $\nabla^2\rho$, and electron localization function ELF at the PBE0/6-311+G*/RECP level.

Name	CP Path	Bond Distances	ρ	H(r)	$\nabla^2\rho$	ELF
C_2 $[Ac@B_{39}]^{2+}$	1	2.987	0.02694	-0.00097	0.06686	0.134
	2	2.815	0.03388	-0.00387	0.07179	0.179
	3	3.012	0.02672	-0.00123	0.06130	0.147
	4	2.815	0.03388	-0.00387	0.07179	0.179
	5	3.012	0.02672	-0.00123	0.06130	0.147
	6	2.987	0.02694	-0.00097	0.06685	0.134

Table S4. In the QTAIM analysis of C_2 $[Th@B_{39}]^{3+}$, ρ, H(r), $\nabla^2\rho$, and ELF at the PBE0/6-311+G*/RECP level.

Name	CP Path	Bond Distances	ρ	H(r)	$\nabla^2\rho$	ELF
C_2 $[Th@B_{39}]^{3+}$	1	2.971	0.03002	-0.00285	0.05971	0.180
	2	2.776	0.03947	-0.00728	0.06586	0.234
	3	2.983	0.03043	-0.00355	0.05351	0.202
	4	2.776	0.03947	-0.00728	0.06586	0.234
	5	2.983	0.03042	-0.00355	0.05351	0.202
	6	2.971	0.03002	-0.00285	0.05971	0.180

Table S5. In the QTAIM analysis of C_2 $Ac@B_{39}$, ρ, H(r), $\nabla^2\rho$, and ELF at the PBE0/6-311+G*/RECP level.

Name	CP Path	Bond Distances	ρ	H(r)	$\nabla^2\rho$	ELF
C_2 $Ac@B_{39}$	1	3.009	0.02621	-0.00061	0.06865	0.122
	2	2.938	0.03032	-0.00235	0.06599	0.168
	3	2.824	0.03376	-0.00369	0.06956	0.187
	4	2.938	0.03032	-0.00235	0.06599	0.168
	5	2.824	0.03376	-0.00369	0.06956	0.187
	6	3.009	0.02621	-0.00061	0.06865	0.122

Table S6. In the QTAIM analysis of C_2 Th@B_{39}, ρ, H(r), $\nabla^2\rho$, and ELF at the PBE0/6-311+G*/RECP level.

Name	CP Path	Bond Distances	ρ	H(r)	$\nabla^2\rho$	ELF
C_2 Th@B_{39}	1	2.990	0.02889	-0.00233	0.06539	0.149
	2	2.772	0.03944	-0.00721	0.06397	0.242
	3	2.908	0.03409	-0.00492	0.05870	0.216
	4	2.772	0.03944	-0.00721	0.06397	0.242
	5	2.908	0.03409	-0.00492	0.05870	0.216
	6	2.990	0.02889	-0.00233	0.06539	0.149

Table S7. The formation energy (kcal/mol) of $[An@B_{39}]^{n+}$ at the PBE0/6-311+G*/RECP level.

Reactions	Formation Energy
$Ac^{3+} + B_{39}^- = [Ac@B_{39}]^{2+}$	-529.1
$Ac^{+} + B_{39}^- = Ac@B_{39}$	-212.5
$Th^{4+} + B_{39}^- = [Th@B_{39}]^{3+}$	-1009.2
$Th^{+} + B_{39}^- = Th@B_{39}$	-296.8